J. Biochem. **138**, 697–700 (2005)
doi:10.1093/jb/mvi167

Characterization of the Protein Phosphatase 1–Binding Motifs of Inhibitor-2 and DARPP-32 by Surface Plasmon Resonance

Ta-Hsien Lin[1,2,3], Pai-Chi Tsai[4], Hsin-Tzu Liu[5], Yi-Chen Chen[6], Lan-Hsin Wang[4], Fu-Kai Hsieh[4] and Hsien-Bin Huang[4,*]

[1]Institute of Biochemistry and Molecular Biology and [2]Structural Biology Program, National Yang-Ming University, Taipei 11221, Taiwan, ROC; [3]Department of Medical Research & Education, Taipei Veterans General Hospital, Taipei 11217, Taiwan, ROC; [4]Institute of Molecular Biology, National Chung Cheng University, Chia-Yi 621, Taiwan, ROC; [5]Department of Research, Buddhist Chi Tzu General Hospital, Hualien 970, Taiwan, ROC; and [6]Department of Medical Technology, Chi Tzu University, Hualien 970, Taiwan, ROC

Received August 25, 2005; accepted September 2, 2005

KLHY is a short amino-acid sequence of inhibitor-2. This sequence is highly conserved with the protein phosphatase 1 (PP1)–binding consensus motif, RVXF. The role of this segment in binding with PP1 is ambiguous. By using surface plasmon resonance we have characterized its binding ability to PP1. Either site-directed mutagenesis or deletion of KLHY did not significantly affect the dissociation constant between PP1 and inhibitor-2. In comparison with DARPP-32, the deletion of KKIQF, a PP1-binding motif of DARPP-32, resulted in a remarkable reduction in its affinity with PP1. Our results suggested that, compared with the common RVXF motif, the KLHY sequence in intact inhibitor-2 binds weakly to PP1.

Key words: inhibitor-2, protein phosphatase-1, surface plasmon resonance.

Inhibitor-1, DARPP-32 (dopamine and cAMP-regulated phosphoprotein, M_r 32,000) and other distinct binding subunits bind to the catalytic subunit of protein phosphatase 1 (PP1) through a conserved motif, RVXF, accounting for their interactions with the enzyme in a mutually exclusive manner (*1–6*). In DARPP-32 this motif is located at residues 7–11, KKIQF. Potent inhibition of PP1 by DARPP-32 requires another contact region, ranging from residue 29 to 35, RRRRPTP, which must be pre-phosphorylated by cAMP-dependent protein kinase (PKA). Either mutation or deletion of KKIQF results in a remarkable reduction in inhibition of PP1.

Inhibitor-2 is also a thermostable protein inhibitor of PP1, and contains residues 144–147, KLHY, which are highly conversed with the RVXF motif. The role of this sequence in interaction with PP1 is ambiguous. Unlike the other PP1-binding proteins, either mutation or deletion of KLHY did not significantly reduce the potency in inhibition of PP1 (*7*). However, a peptide encompassing the residues 135–151 could antagonize the inhibitory potency of inhibitor-2. Antagonization of inhibitor-2 by I2(131–155) disappeared when both Leu-145 and Tyr-147 of the peptide were replaced by Ala, suggesting that KLHY acts as a second site of interaction, corresponding to the conserved RVXF motif (*8*). To gain more insight into the role of the KLHY sequence in association with PP1, we have applied surface plasmon resonance to characterize its binding ability to PP1. For comparison, the binding ability of the PP1-binding motif of DARPP-32 was also characterized by using surface plasmon resonance.

*To whom correspondence should be addressed. Fax: +886-5-272-2871, E-mail: Biohbh@ccu.edu.tw

MATERIALS AND METHODS

Materials—Tris, EDTA, HEPES, 2-mercaptoethanol and ATP were obtained from Sigma. Iodoacetyl-LC-biotin and TCEP-HCl were purchased from Pierce. The catalytic subunit of PP1 was purified from rabbit skeletal muscle as described (*9*). The recombinant PP1α was prepared as described (*10*). The purified native and recombinant PP1s were intact forms without C-terminal truncation, as judged by SDS-PAGE (data not shown). The recombinant wild-type and mutants of human inhibitor-2, I2[1–160] and I2[1–140], were prepared as described (*7*). The recombinant rat DARPP-32 and D32Δ[6–11] were prepared as described (*7*). Phosphorylation of DARPP-32 by PKA followed the method as described (*2*).

Preparations of Biotin-Conjugated Inhibitor-2 and Biotin-Conjugated DARPP-32—Human inhibitor-2 contains a single cysteine at residue 85, and this was reacted with iodoacetyl-LC-biotin (*11*). All reaction components contained 0.45 M Tris-HCl buffer at pH 8.6, wild-type or inhibitor-2 mutant (4 mg/ml), guanidine hydrochloride (6 M), EDTA (0.2 mM), TCEP (10 mM), and iodoacetyl-LC-biotin (4 mg/ml). The reaction was carried out at room temperature for 20 min, followed by gel filtration on G-25, developed with 0.2 M acetic acid, to remove the excess reagents. The fractions containing the biotin-conjugated inhibitor-2 (or biotin-conjugated inhibitor-2 mutant) were pooled and lyophilized to powder. Biotin conjugation on Cys-85 did not affect inhibitor-2 in inhibition of PP1 (data not shown). Rat DARPP-32 contains a single cysteinyl residue at position 72. Preparation of biotin-conjugated DARPP-32 followed the method as mentioned above.

Surface Plasmon Resonance Analysis—Surface plasmon resonance measurements were performed on a BIACORE 3000 (Pharmica, Sweden). All biotin-conjugated inhibitors,

including wild-type, mutated inhibitor-2 and phospho-DARPP-32 (or phospho-D32Δ[6–11]), were immobilized onto a streptavidin-coated sensor chip in HBS-EP buffer (10 mM HEPES, 150 mM NaCl, 3 mM EDTA, 0.005% polysorbate 20 at pH 7.4) at a concentration of 5 μM with a flow-rate of 2 μl/min until the resonance unit reached a steady state. The unbound protein was then washed off by injecting 10 mM $NaHCO_3$ buffer at a flow-rate of 30 μl/min until the curves reached a steady state. For the dissociation constant (K_D) measurements, PP1 at concentrations ranging from 2.5 to 60 nM was injected through the channel at a flow rate of 30 μl/min for 150 s to induce the binding, followed by injection of HBS-EP buffer in the absence of PP1 with the same flow-rate for 480 s for dissociation. After each cycle, the remainder of bound PP1 was removed by washing with 10 mM $NaHCO_3$ buffer at the flow-rate of 30 μl/min for 40 s. Association and dissociation kinetic rate constants (k_{on} and k_{off}) and the equilibrium dissociation constant, K_D, were calculated using BIAevaluation 3.0 software (Pharmica, Sweden). The fitting model for all curves used 1:1 binding with drifting baseline. In order to fit the experimental data precisely, the value of χ^2, representing the mean square of the signal noise, for each fitting must be less than 5. The concentration of the native PP1, purified from rabbit muscles, was estimated from the optic density of the enzyme on SDS-PAGE by using bovine serum albumin as the standard. The concentration of the recombinant PP1α was estimated by UV spectrophotometry at 280 nm, at which the absorbance of 1 mg/ml enzyme was equal to 1.0825 (*10*).

RESULTS AND DISCUSSION

Measurement of the Dissociation Constants for Binding of PP1 to Inhibitor-2 and Its Mutant by Surface Plasmon Resonance—If the $K_{144}LHY_{147}$ sequence of inhibitor-2 strongly binds to PP1, the interaction between this sequence and PP1 should make a major contribution to the binding affinity. Either site-directed mutagenesis or deletion of this sequence would then result in a significant decrease in binding affinity. In order to test this inference, we measured the dissociation constants by surface plasmon resonance for PP1 in the presence of wild-type inhibitor-2 and mutant I2[Y147A]. Biotin-conjugated inhibitor-2 was immobilized on a streptavidin-coated sensor chip. As the recombinant PP1 was injected to the immobilized inhibitor-2, the resonance unit increased initially and reached its equilibrium state as depicted in Fig. 1A. Switching the injection to HBS-EP buffer in the absence of PP1 resulted in the dissociation of PP1 from the complex, leading to a decrease in the resonance unit. From these dissociation curves at different concentrations, the k_{on} and k_{off} rate constants were obtained. The equilibrium constants (K_D) were calculated from the ratio of k_{on}/k_{off}. The K_D values, averaged from six independent measurements, for PP1 in dissociation with the wild-type I2 is 1.8 ± 1.6 nM, a result very similar to that obtained from fluorescence studies (*12*). K_D is highly correlated with IC_{50} value (data not shown).

The curves for mutant I2[Y147A] binding to and dissociating from the immobilized PP1 are somewhat different from those of wild-type inhibitor-2 (Fig. 1B). The dissociation rate of I2[Y147A] is faster than that of wild-type,

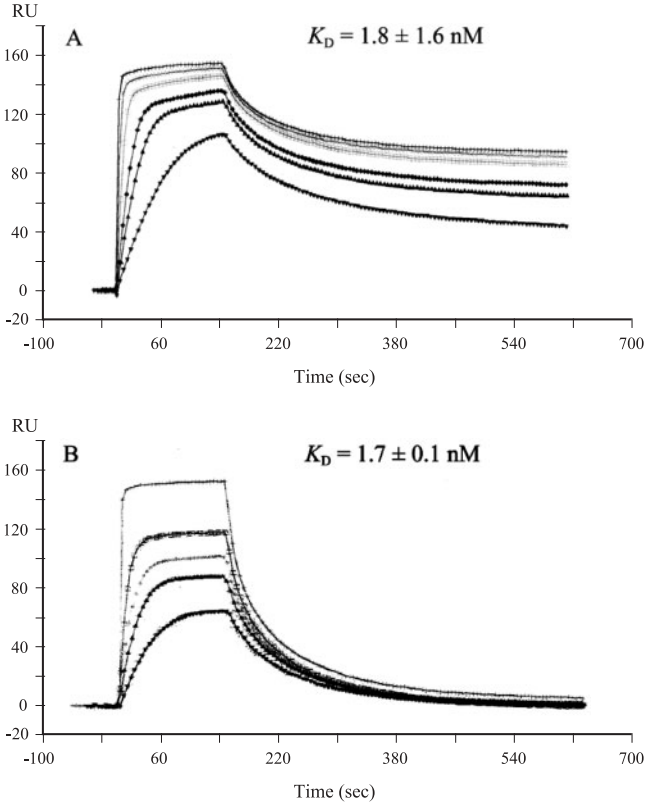

Fig. 1. **Surface Plasmon Resonance analysis of binding of recombinant PP1 to wild-type inhibitor-2 and to mutant I2[Y147A].** The recombinant PP1 was used for injection. The curves represent the concentrations of the injected PP1. From bottom to top: 2.5, 5, 7.5, 15, 30 and 60 nM. The biotin-conjugated proteins immobilized on the streptavidin-coated sensor chip are the wild-type (A) and I2[Y147A] (B).The K_D values are expressed as mean ± SD, n = 6 for the wild-type and n = 3 for I2[Y147A] and obtained from an average of each experimental measurement of k_{on}/k_{off}. RU: Resonance unit.

Table 1. **The association kinetic rate (k_{on}) and dissociation kinetic rate (k_{off}) for recombinant PP1 binding to and dissociating from the immobilized inhibitor-2 and I2[Y147A].** Both k_{on} and k_{off} values were obtained from the fitting curves of the experimental measurements in Fig. 1, A and B. The values are expressed as mean ± SD, n = 6 for the wild-type and n = 3 for I2[Y147A].

Substrate	k_{on} (M^{-1} s^{-1})	k_{off} (s^{-1})
Wild-type I2	$3.99 \pm 3.25 \times 10^6$	$3.48 \pm 0.69 \times 10^{-3}$
I2[Y147A]	$7.20 \pm 0.94 \times 10^6$	$1.19 \pm 0.05 \times 10^{-2}$

reflecting on the fact that more than 90% of I2[Y147A] is dissociated from the immobilized PP1 at 620 s, but less than 50% of wild-type is dissociated under the same conditions (Fig. 1, A and B). Mutation of Tyr-147 to Ala also resulted in a change in the k_{on} value. Table 1 shows the k_{on} and k_{off} values for the recombinant PP1 binding to and dissociating from the immobilized inhibitor-2 and I2[Y147A]. The k_{on} values for wild-type inhibitor-2 and I2[Y147A] are $3.99 \pm 3.25 \times 10^6$ and $7.20 \pm 0.94 \times 10^6$ (M^{-1} s^{-1}), respectively, while the k_{off} values are $3.48 \pm 0.69 \times 10^{-3}$ and $1.19 \pm 0.05 \times 10^{-2}$, respectively. Although replacement of Tyr-147 by Ala of inhibitor-2 resulted in increases of both k_{on} and

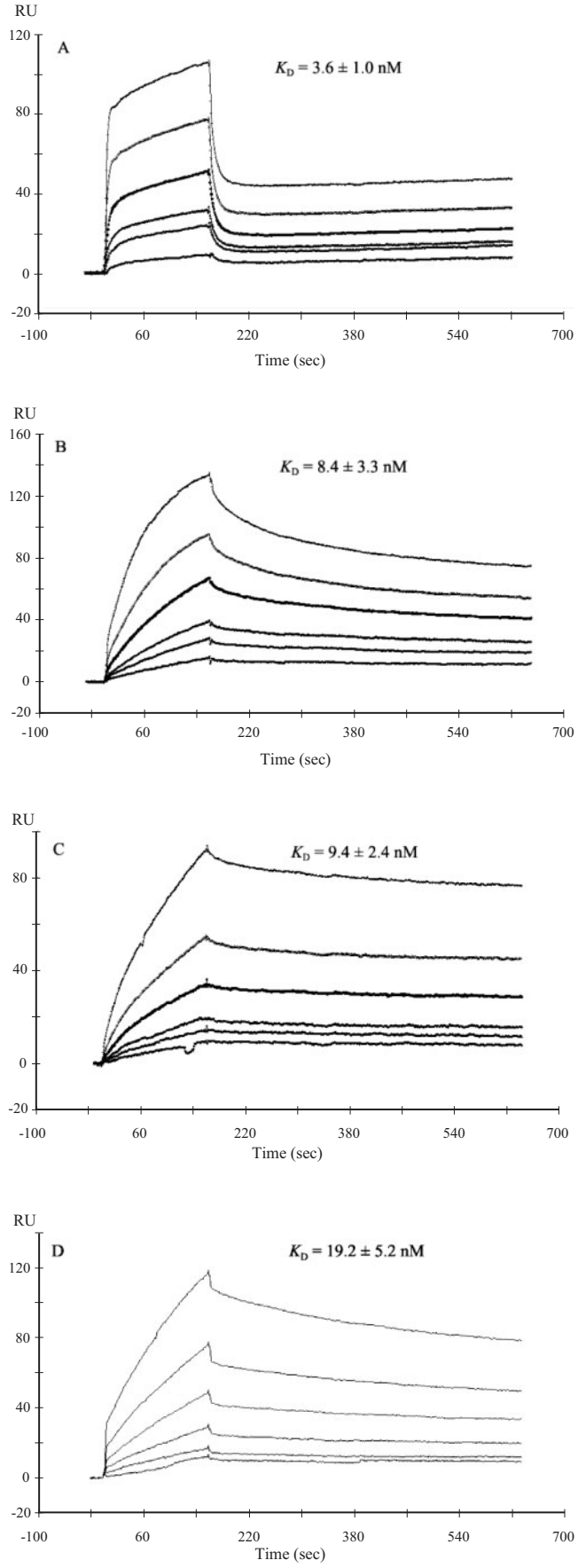

k_{off}, the dissociation constant (K_D) estimated from the ratio of k_{on}/k_{off} did not change significantly (Fig. 1, A and B).

To fully explore the role of KLHY in inhibition of PP1, we also measured the K_D for truncated I2[1–160] and I2[1–140] with native PP1. Here, the reason for using native PP1 is that a 40-amino-acid deletion from the COOH terminus of inhibitor-2 could result in an increase in the IC_{50} value by one order of magnitude in the inhibition assay for the recombinant PP1 (data not shown), although the IC_{50} values obtained for the inhibition of the native and the recombinant PP1 by the wild-type inhibitor-2 are similar (data not shown). Table 2 shows the k_{on} and k_{off} values for the native PP1 binding to and dissociating from the immobilized inhibitor-2, I2[1–160] and I2[1–140]. The K_D values, calculated from Table 2, for the native PP1 binding to the immobilized wild-type I2, I2[1–160] and I2[1–140] are 3.6 ± 1.0, 8.4 ± 3.3 and 9.4 ± 2.4 nM, respectively, suggesting that deletion of 44 and 64 COOH-terminal amino acids had a slight effect on the binding of inhibitor-2 to PP1 (Fig. 2, A, B and C). Previous study had indicated that the sequence $I_{10}KGI_{13}$ directly binds to the enzyme. The IC_{50} value was obviously increased by one order when Ile-13 of inhibitor-2 was replaced by Ala (7). In our measurement, the K_D value for the native PP1 binding to I2[I13A] was also increased by almost one order, to 19.2 ± 5.2 nM (Fig. 2D). This result further supports the notion that the KLHY sequence in intact I2 has a little effect on binding to PP1. However, mutation at the PP1-binding site, $I_{10}KGI_{13}$, of inhibitor-2 results in a significant decrease in k_{on} value, but no effect on k_{off} (Table 2).

Analysis of the Binding of PP1 to Phospho-DARPP-32 by Surface Plasmon Resonance—In DARPP-32 the RVXF motif is located at residues 7–11, KKIQF. The KLHY sequence in I2 has been proposed to have the same role as the KKIQF sequence in DARPP-32 (*8*). Thus, the behavior of binding affinity with PP1 resulting from deletion of the KKIQF sequence in DARPP-32 should be very similar to that resulting from deletion of the KLHY sequence in I2. This can be demonstrated by measuring the dissociation constants for native PP1 binding to phospho-DARPP-32 with and without its KKIQF motif being deleted. The biotin-labeled phospho-DARPP-32 was immobilized onto a streptavidin-coated sensor chip. Continuously applying the native PP1 (30 nM) to the immobilized phospho-DARPP-32 resulted in an increase in the resonance unit until the equilibrium stage was reached. At this point, injection of HBS-EP buffer induced the dissociation and resulted in a decrease in the resonance unit (Fig. 3). In contrast, under the same conditions, the native PP1 weakly bound to the immobilized D32Δ[6–11], in which the KKIQF motif had been deleted. Even when the concentration of the injected enzyme was increased to 240 nM, the resonance unit remained at the background

Fig. 2. **Surface Plasmon Resonance analysis of binding of native PP1 to wild-type inhibitor-2, I2[1–160], I2[1–140] and I2[I13A].** The native PP1 purified from rabbit skeletal muscles was used for injection. The curves represent the concentrations of the injected PP1. From bottom to top: 2.5, 5, 7.5, 15, 30 and 60 nM. The biotin-conjugated proteins immobilized on the streptavidin-coated sensor chip are the wild-type (A), I2[1–160] (B), I2[1–140] (C), and I2[I13A] (D). The K_D values are expressed as mean ± SD, n = 3. RU: Resonance unit.

Table 2. **The association kinetic rate (k_{on}) and dissociation kinetic rate (k_{off}) for native PP1 binding and dissociating from the immobilized inhibitor-2, I2[1–160], I2[1–140] and I2[I13A].** Both k_{on} and k_{off} values were obtained from the fitting curves of the experimental measurements in Fig. 2, A–D. The values are expressed as mean ± SD, $n = 3$.

Substrate	k_{on} (M^{-1} s^{-1})	k_{off} (s^{-1})
Wild-type I2	$(3.0 \pm 1.3) \times 10^5$	$(1.2 \pm 0.7) \times 10^{-3}$
I2[1–160]	$(2.7 \pm 0.4) \times 10^5$	$(2.3 \pm 1.0) \times 10^{-3}$
I2[1–140]	$(1.2 \pm 0.2) \times 10^5$	$(1.1 \pm 0.1) \times 10^{-3}$
I2[I13A]	$(7.5 \pm 1.4) \times 10^4$	$(1.4 \pm 0.2) \times 10^{-3}$

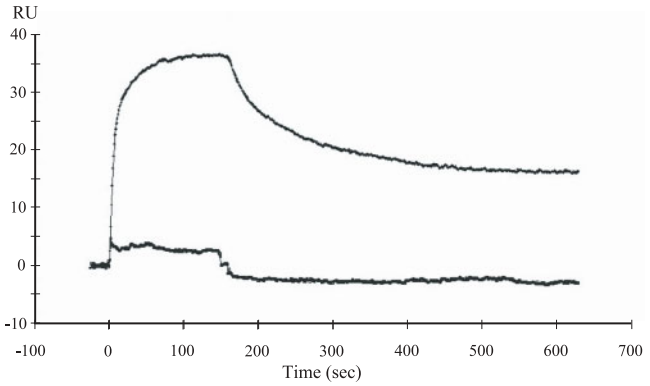

Fig. 3. **Surface Plasmon Resonance analysis of binding of PP1 to phospho-DARPP-32 and phospho-D32Δ(6–11).** The top curve represents 30 nM PP1 purified from rabbit skeletal muscle injected over the immobilized phospho-DARPP-32 sensor chip; the bottom curve represents 240 nM PP1 injected over the immobilized phospho-D32Δ(6–11) sensor chip.

level (Fig. 3). This result suggests that deletion of the PP1-binding motif leads to a significant decrease in binding affinity. Comparison of the dissociation constants between DARPP-32 and I2 demonstrates that the KLHY motif in intact I2 does not bind or only weakly binds to PP1.

Our previous studies have clearly indicated that mutating Phe-11 to Ala or deletion of the R_6KKIQF_{11} sequence from phospho-DARPP-32 caused a significant increase in IC_{50} (*7*). The results from the present study demonstrate that deletion of the RKKIQF sequence of DARPP-32 results in a significant reduction in the binding affinity with PP1. Apparently, abolition of the RKKIQF-binding results in a reduction of inhibitory potency. A similar result for another PP1 regulatory protein, spinophilin, which targets PP1 to dendritic spines, was also obtained (*13*). The PP1-binding motif of spinophilin is located within residues 447–451, RKIHF. Replacement of Phe-451 by Ala or deletion of the RKIHF sequence abrogated the ability of spinophilin to associate with PP1. This evidence makes it clear that the role of RVXF motif is the main association site for all PP1-binding proteins to bind to the enzyme. However, in the present study, the KLHY sequence of inhibitor-2 does not show such a function. Dissociation constant measurements have clearly demonstrated that the sequence KLHY functions for weak binding, compared with the common PP-binding motif, RVXF.

This work was supported by Grants from the National Science Council of the Republic of China (NSC 92-2320-B-194-005 and NSC 92-2311-B-010-003), the Taipei Veterans General Hospital Taiwan, Republic of China.

REFERENCES

1. Cohen, P.T.W. (2002) Protein phosphatase 1-targeted in many directions. *J. Cell Sci.* **115**, 241–256
2. Hemmings, H.C., Jr., Nairn, A.C., Eilliott, J.I., and Greengard, P. (1990) Synthetic peptide analogs of DARPP-32 (Mr. 32,000 dopamine- and cAMP-regulated phosphoprotein), an inhibitor of protein phosphatase-1. Phosphorylation, dephosphorylation, and inhibitory activity. *J. Biol. Chem.* **265**, 20369–20376
3. Desdouits, F., Cheetham, J.J., Huang, H.B., Kwon, Y.G., da Cruze Silva, E.F., Denefle, P., Ehrlich, M.E., Nairn, A.C., Greengard, P., and Girault, J.A. (1995) Mechanism of inhibition of protein phosphatase 1 by DARPP-32: studies with recombinant DARPP-32 and synthetic peptides. *Biochem. Biophys. Res. Commun.* **206**, 652–658
4. Endo, S., Zhou, X., Connor, J., Wang, B., and Shenolikar, S. (1996) Multiple structural elements define the specificity of recombinant human inhibitor-1 as a protein phosphatase-1 inhibitor. *Biochemistry* **35**, 5220–5228
5. Kwon, Y.G., Huang, H.B., Desdouits, F., Girault, J.A., Greengard, P., and Nairn, A.C. (1997) Characterization of the interaction between DARPP-32 and protein phosphatase 1 (PP1): DARPP-32 peptides antagonize the interaction of PP1 with binding proteins. *Proc. Natl. Acad. Sci. USA* **94**, 3536–3541
6. Egloff, M.P., Johnson, D.F., Moorhead, G., Cohen, P.T.W., Cohen, P., and Barford, D. (1997) Structural basis for the recognition of regulatory subunits by its catalytic subunit of protein phosphatase 1. *EMBO J.* **16**, 1876–1887
7. Huang, H.B., Horiuchi, A., Watanabe, T., Shih, S.-R., Tsay, H.-J., Li., H.C., Greengard, P., and Nairn, A.C. (1999) Characterization of the inhibition of protein phosphatase-1 by DARPP-32 and inhibitor-2. *J. Biol. Chem.* **274**, 7870–7878
8. Yang, J., Hurley, T.D., and DePaoli-Roach, A.A. (2000) Interaction of inhibitor-2 with catalytic subunit of type 1 protein phosphatase. *J. Biol. Chem.* **275**, 22635–22644
9. Cohen, P., Alemany, S., Hemmings, B.A., Resink, T.J., Stralfors, P., and Tung, H.Y. (1988) Protein phosphatase-1 and protein phosphatase-2A from rabbit skeletal muscle. *Methods Enzymol.* **159**, 390–408
10. Goldberg, J., Huang, H.B., Kwon, Y.G., Greengard, P., Nairn, A.C., and Kuriyan, J. (1995) Three-dimensional structure of the catalytic subunit of protein serine/threonine phosphatase-1. *Nature* **376**, 745–753
11. Helps, N.R., Street, A.J., Elledge, S.J., and Cohen, P.T.W. (1994) Cloning of the complete coding region for human protein phosphatase inhibitor-2 using the two hybrid system and expression of inhibitor-2 in *E. coli*. *FEBS Lett.* **340**, 93–98
12. Picking, W.D., Kudlicki, W., Kramer, G., Hardesty, B., Vandenheede, J.R., Merlevede, W., Park, I.K., and DePaoli-Roach, A. (1991) Fluorescence studies on the interaction of inhibitor-2 and okadaic acid with the catalytic subunit of type-1 phosphoprotein phosphatases. *Biochemistry* **30**, 10280–10287
13. Hsieh-Wilson, L.C., Allen, P.B., Watanabe, T., Nairn, A.C., and Greengard, P. (1999) Characterization of the neuronal targeting protein spinophilin and its interactions with protein phosphatase-1. *Biochemistry* **38**, 4365–4373